JOURNAL OF GEOPHYSICAL RESEARCH, VOL. 97, NO. D17, PAGES 18,523–18,531, NOVEMBER 30, 1992

FIFE Atmospheric Boundary Layer Budget Methods

A. K. BETTS

Atmospheric Research, Middlebury, Vermont

The budget methods and the mixed layer model used to analyze the aircraft data from the First ISLSCP Field Experiment (FIFE) are outlined. The separation of the temporal and horizontal derivatives is discussed. Vector budgets for the mixed layer are presented on conserved variable diagrams. Theoretical solutions are given for the critical surface Bowen ratio, which produces no boundary layer moistening or equivalent potential temperature rise as a function of the Bowen ratio at the inversion. Improved measurement strategies are suggested.

INTRODUCTION

This paper discusses the budget methods used to analyze aircraft data during the First International Satellite Land Surface Climatology Project (ISLSCP) Field Experiment (FIFE). FIFE included an extensive program of surface and atmospheric boundary layer (ABL) measurements in order to develop techniques to measure the exchange of momentum, heat, moisture, and CO_2 between the Earth's surface and the atmosphere. The boundary layer aircraft flights were designed to compare fluxes and budgets for the ABL with surface measurements of sensible and latent heat flux and CO_2. The ABL flights in FIFE had three interrelated objectives. The first was to compare flux measurements from distributed surface sites with vertical flux profiles from aircraft flying repeated 15 km legs. The second was to attempt a volumetric budget of the ABL to assess the importance of horizontal advection terms and to derive mean surface fluxes for the FIFE area as budget residuals for a relatively homogeneous grassland ecosystem. The third was to study ABL top entrainment fluxes and to check the validity of simple mixed layer models for the ABL. The FIFE flights concentrated on clear days when neither clouds nor precipitation affected the grassland photosynthesis and evapotranspiration. The surface portable automated mesonet (PAM) data were used to define the mean surface time trend for the FIFE area, and the frequent sounding data were used to define ABL depth and the Bowen ratio at the ABL top inversion.

The three basic flight plans are shown in Figure 1. The "L"-shaped pattern, shown in Figure 1*a*, consisted of north-south and east-west legs flown in both directions at several altitudes. On occasion a "T"-shaped pattern was flown. Figure 1*b* shows the double-stack pattern, consisting of vertical sequences of stacks at the north and south end of the FIFE area [see *Betts et al.*, 1990]. Figure 1*c* shows the "grid" pattern flown at a single low altitude (75–100 m) to study spatial variability of ABL structure and fluxes [*Betts et al.*, this issue]. The arrow shows the direction of a southerly wind. During the early phases of FIFE in 1987 a simpler east-west single-stack pattern was frequently flown across the wind, usually crossing over one of the surface eddy correlation flux sites.

Paper number 91JD03172.
0148-0227/92/91JD-03172$05.00

BUDGET METHOD

This paper focuses on the budget methods used in the FIFE ABL analysis.

Budget Equations

Consider a scalar ξ for which there are no sources and sinks in the boundary layer. This satisfies the conservation equation

$$D\xi/Dt = \partial\xi/\partial t + \mathbf{v}\cdot\nabla\xi = 0 \qquad (1a)$$

This can be rewritten, using the continuity equation

$$\nabla(\bar{\rho}\mathbf{v}\xi) = 0$$

where ρ is mean air density, as

$$\bar{\rho}\,\partial\xi/\partial t + \nabla(\bar{\rho}\mathbf{v}\xi) = 0 \qquad (1b)$$

Equation (1*b*) can be expanded in terms of horizontal averages and deviations to give, after rearrangement,

$$\bar{\rho}[\partial\bar{\xi}/\partial t + \bar{u}\partial\bar{\xi}/\partial x + \bar{v}\partial\bar{\xi}/\partial y + \bar{w}\partial\bar{\xi}/\partial z + \partial(\overline{u'\xi'})/\partial x + \partial(\overline{v'\xi'})/\partial y] + \partial(\overline{w'\xi'})/\partial z = 0 \qquad (2a)$$

where u, v and w are the three wind components in the x, y, and z directions, oriented in the conventional meteorological directions: to the east, north, and upward, respectively. Equation (2*a*) has a time rate of change term, mean advection terms, and eddy transports by the boundary layer turbulence. Overbars denote horizontal averaging, and primes denote deviations from the horizontal average. In the FIFE budget studies the horizontal divergence of the horizontal eddy fluxes were found to be small on the basis of estimates made using aircraft data, and they were therefore neglected. Equation (2*a*) then reduces to (2*b*):

$$\bar{\rho}(\partial\bar{\xi}/\partial t + \bar{u}\partial\bar{\xi}/\partial x + \bar{v}\partial\bar{\xi}/\partial y + \bar{w}\partial\bar{\xi}/\partial z) + \partial(\overline{\rho\, w'\xi'})/\partial z = 0 \qquad (2b)$$

During the daytime over land the boundary layer is being driven by the large surface fluxes of heat and moisture. The surface fluxes generate convective turbulence, which in turn drives large entrainment fluxes at the top of the ABL and results in the deepening of the ABL with time. The vertical gradient of these vertical eddy fluxes (the last term in equation (2*b*)) is large, and as a result the ABL has a large time dependence (the first term) during the daytime under

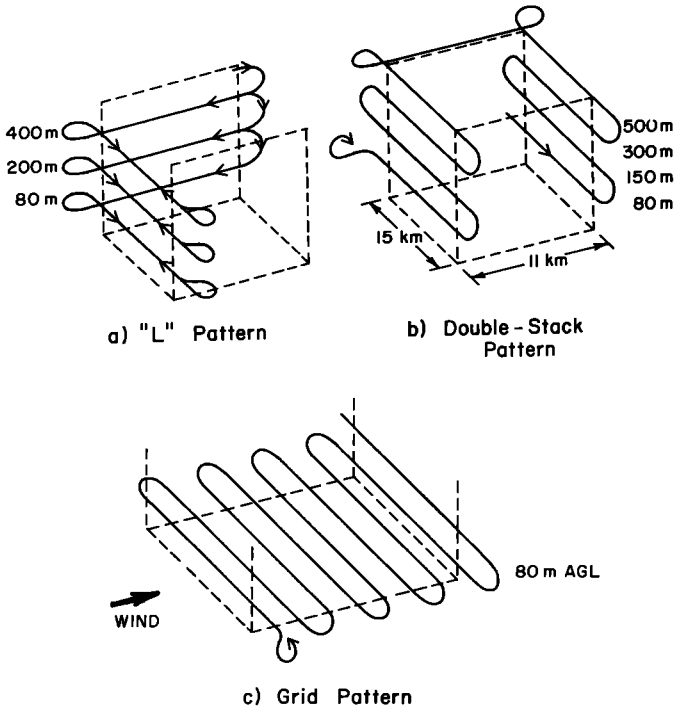

Fig. 1. FIFE atmospheric boundary layer (ABL) flight plans. The arrow shows a typical southerly wind direction.

clear skies. However, the two mean horizontal advection terms are often not negligible: they represent the change to the mean ABL from warm (or cold), moist (or dry) advection into the FIFE area. The vertical advection $\bar{w}\partial\bar{\xi}/\partial z$ is hard to measure. Estimates showed it to be an order of magnitude smaller than any other term, both because $\bar{w}$ (estimated from the horizontal divergence) was small and because $\partial\bar{\xi}/\partial z$ is generally small within a nearly mixed ABL. For now, the vertical advection term is retained. In the subsequent analysis it will be incorporated into the entrainment term at the top of the ABL.

Conserved Variables

The two conserved variables used for the budget analyses of the FIFE ABL were dry potential temperature, θ, and mixing ratio, q. Mean budgets for the mixed ABL were generated. The aircraft flight level data were used to generate mixed layer means [*Betts et al.*, 1990], whenever stack patterns were flown with several levels in the vertical (Figures 1*a* and 1*b*). For the grid pattern flights [*Betts et al.*, this issue] only a single level was flown at about 80 m above ground level (Figure 1*c*), and the mean data at this level (near the top of the surface superadiabatic layer) were taken as representative of a mixed layer mean. *Betts et al.* [1990] showed this to be a good assumption.

Vertical Flux Gradients

For the aircraft patterns with flight legs at several levels (Figures 1*a* and 1*b*), the last term in (2*b*), the vertical flux divergence, can be estimated directly. This gradient is a crucial one, since it is driving the time dependence of the ABL. It can be used to extrapolate the fluxes to the top of the ABL, where the turbulent mixing at the inversion is typically forcing the mixing or entrainment of warm dry air from above the capping inversion. This downward mixing of warm dry air means that the convective fluxes at the top of the mixed layer are typically a downward flux of θ and an upward flux of q. Because the daytime evolution of the ABL depends on both the surface fluxes and these inversion level entrainment fluxes, a key FIFE objective was to test the validity of mixed layer models for the ABL, in which the inversion level fluxes are usually parameterized. For the grid paterns in Figure 1*c* there are no height gradients from the aircraft, and a mixed layer model was used to determine the vertical flux gradients.

In the work of *Betts et al.* [1990] the vertical flux gradients were also determined by using the surface site data and the highest level aircraft data. The mean surface fluxes over the FIFE area were found by averaging the 30-min mean values from the surface flux sites [*Smith et al.*, this issue]; and then interpolating and averaging these area means for the time period of each aircraft flight. Because of filtering, the aircraft fluxes, extrapolated to the surface, were consistently less than the surface site average fluxes, except for the small latent heat fluxes in October [*Betts et al.*, this issue].

Separation of Time and Horizontal Space Derivatives in Aircraft Data

Surface PAM stations were deployed during FIFE. These give a representative time derivative in the surface layer, but it is not easy to extract weak horizontal gradients from the mesonet because of variations among sites and instruments. In contrast, the aircraft measurements are from a single platform within the mixed layer. However, at flight speeds of 50–100 m s^{-1}, each pattern takes 1–2 hours of flight time, and time and spatial derivatives are intermixed in the data. For the budget studies we needed to separate the time and space gradients.

The gradients along the flight track can be determined by averaging the trend lines for a set of legs, provided a sufficient number of legs were flown at one level. Although the time derivative can be significant for each leg (typically approximately 3 min in length), the legs were flown in pairs in opposite directions, so that the time derivative approximately cancels in the pattern average. For the grid flights we have a set of 16 legs which cover the whole FIFE area, but for the L and stack patterns the legs are fewer and they are only at edges of the FIFE area, so we must assume they are representative of the whole area. The L patterns gave an estimate of both x and y gradients and hence both advection terms, but *Grossman* [this issue] questions whether the assumption of representativity is valid. Some of the FIFE 1987 L patterns have not yet been analyzed.

To separate the cross-leg, typically the north-south (y) gradient for the patterns in Figures 1*b* and 1*c* from the time derivative, we assume constant gradients in both time and space during the pattern. This is a restrictive assumption which is not always satisfied [*Betts et al.*, this issue]. The stack pattern (Figure 1*b*) was flown in a time-centered fashion, so that the average time of each pair of legs was nearly the same; and corrections can be made using the time trend for small offsets in time. *Betts et al.* [this issue] found that estimating the north-south advection from the two pairs of stacks near the north and south ends of the FIFE area was possible. However, they also found that the method had

large errors, because the spacing of the stacks was only 11 km, and the north-south (v) wind component was often large ($\approx$10 m s^{-1}). In high winds the advection time over the site is only 15–20 min. *Betts et al.* [this issue], in analyzing the grid flights, used linear regression in time and the y direction to separate these gradients. They found encouraging results, although the assumption of linearity in time was not satisfied for nearly half the flights. In particular, $\theta(t)$ has marked curvature during and after the surface temperature maximum. For flights at these times the curvature in $\theta(t)$ introduces bias into the estimate of the north-south advection. When linear regression is applied to a pattern flown from north to south and then back, it converts a quadratic θ dependence in time into its linear component and a spurious spatial gradient $\partial\bar{\theta}/\partial y$. The mean time variation from the PAM stations was used to determine when linearity in time was clearly not satisfied. On occasion, time changes were due to sudden changes in fluxes at the inversion, as dry layers above appeared or disappeared. In these cases the sounding data showed changes in the Bowen ratio at the inversion.

MIXED LAYER MODEL

Although there are weak gradients of θ and q above the surface superadiabatic layer, the main characteristic of the dry ABL is that it is almost well mixed in θ and q. Recognizing this, *Betts* [1973], *Tennekes* [1973], and *Carson* [1973] defined similar integral mixed layer model simplifications for the ABL by integrating (2b) from the surface to the inversion base at a height Z_i. If we define a layer average as [*Deardorff et al.*, 1974]

$$\langle\bar{\xi}\rangle \equiv (1/\langle\bar{\rho}\rangle Zi)\int_0^{Z_i}\bar{\xi}\bar{\rho}\,dz \tag{3}$$

then the mixed layer average budgets can be written as

$$\partial\langle\bar{\xi}\rangle/\partial t + \langle\bar{u}\partial\bar{\xi}/\partial x\rangle + \langle\bar{v}\partial\bar{\xi}/\partial y\rangle = (\bar{\rho}\overline{w'\xi'_s} - \bar{\rho}\overline{w'\xi'_i})/\langle\bar{\rho}\rangle Z_i + \bar{\rho}(\partial Z_i/\partial t - \bar{w}_i)(\bar{\xi}_i - \langle\bar{\xi}\rangle)/\langle\bar{\rho}\rangle Z_i \tag{4}$$

where the subscripts s and i denote values at the surface and inversion base, respectively. The last term on the right-hand side has two components that deserve discussion, because the interpretation of our budget results involve a subtle interplay between observations and the model mixed layer assumption. This was recognized when the model was first introduced [*Deardorff et al.*, 1974; *Betts*, 1974], but this analysis has not been included subsequently in textbooks such as *Stull*'s [1988], so some confusion exists. The term $\partial Z_i/\partial t\ (\bar{\xi}_i - \langle\bar{\xi}\rangle)$ comes from differentiating (3), which defines $\langle\bar{\xi}\rangle$ up to a moving boundary Z_i, which increases as the ABL deepens. The corresponding term in w_i comes from the integration of the subsidence term $\bar{w}\partial\bar{\xi}/\partial z$ in (2b), with the small approximation of constant divergence below Z_i. Together, these terms can be written as an entrainment term

$$\bar{\rho}W_e(\bar{\xi}_i - \langle\bar{\xi}\rangle) \tag{5}$$

where $W_e = (\partial Z_i/\partial t - \bar{w}_i)$ is the deepening of the layer by entrainment.

The choice of the level Z_i is important to the conceptual analysis. Convectively mixed boundary layers have a capping inversion, a transition or interfacial layer [*Deardorff*, 1979; *Ludlam*, 1980], which separates the fully turbulent layer below from the stably stratified and relatively nonturbulent free atmosphere above. If we choose Z_i at the top of this inversion, say, Z_i^+, then $\overline{w'\xi'}_i = 0$, and the budget equation (4) contains only the entrainment term. This term can be written $W_e\Delta\bar{\xi}$, where $\Delta\bar{\xi} = \bar{\xi}_i^+ - \langle\bar{\xi}\rangle$ is the jump in $\bar{\xi}$ from the mixed layer to the ABL top, where the turbulent fluxes go to zero or are greatly reduced. In this paper, however, the entrainment term will not be split into these components. If we choose Z_i at the base of the inversion, say, Z_i^-, then $\bar{\xi}_i^- - \langle\bar{\xi}\rangle$ is typically small, and $\overline{w'\xi'_i}$ is the larger term [*Betts*, 1974]. Capping inversions in the atmosphere are associated with strong divergence in the vertical turbulent flux of heat [*Betts*, 1974; *Deardorff*, 1979]. If the mixed layer were truly well mixed, with constant $\bar{\xi} = \langle\bar{\xi}\rangle$ up to Z_i^-, then the term denoted (5) disappears below the inversion and the fluxes $\overline{w'\xi'}$ are linear between the surface and Z_i^-, where the heat flux reaches its maximum negative value [*Deardorff et al.*, 1974]. In the FIFE data (unlike the laboratory measurements discussed by *Deardorff et al.* [1974]), we have no reliable measurements of $\overline{w'\xi'}$ at the inversion base. The estimates of the inversion level fluxes that come either from linear extrapolation up to some level Z_i^-, or from the budget method, use the mixed layer model. Consequently, they are not what an aircraft might measure at Z_i^- (if the sampling problems could be resolved), but a parametric representation of the total effect of the entrainment process on the evolution of the mean layer below the inversion base. Formally, we reduce (4) to

$$\partial\langle\bar{\xi}\rangle/\partial t + \langle\bar{u}\partial\bar{\xi}/\partial x\rangle + \langle\bar{v}\partial\bar{\xi}/\partial y\rangle = \langle F_{s\xi} - F_{i\xi}\rangle/\langle\bar{\rho}\rangle Z_i \tag{4'}$$

where $F_{s\xi} = \bar{\rho}\overline{w'\xi'_s}$ and $F_{i\xi} = \bar{\rho}\overline{w'\xi'_i} + \bar{\rho}W_e(\bar{\xi}_i - \langle\bar{\xi}\rangle)$.

The fluxes represented by $F_{i\xi}$ are the equivalent mixed layer fluxes at the inversion base, and it is these that are determined by our analysis. In this way the mixed layer model formally includes the effects of the stratification within the ABL, coupled to the subsidence and boundary layer growth, as part of the entrainment fluxes that are typically warming and drying the mixed layer.

For flight patterns where we have several layers in the vertical, we can approximate the mixed layer averages. In fact, we used simple averages of all aircraft levels. Typically, the gradients at any one level of $\partial\bar{\xi}/\partial x$ and $\partial\bar{\xi}/\partial y$ are not accurately known, so we also simplified the mean advection terms to $\langle\bar{u}\rangle\partial\langle\bar{\xi}\rangle/\partial x$. Linear regression can give a mean value of $\langle\partial\bar{\rho}\overline{w'\xi'}/\partial z\rangle$, and this value can be used to extrapolate either down to the surface or up to the inversion base Z_i. Extrapolation of the aircraft flux profiles to the surface quickly showed that the aircraft appear to underestimate the low level fluxes [*Betts et al.*, 1990, this issue; *Kelly et al.*, this issue]. These results are summarized later. As discussed earlier, extrapolation of the aircraft fluxes up to the inversion height Z_i gives an estimate of the equivalent inversion entrainment fluxes $F_{i\xi}$ in (4′). These were compared by *Betts et al.* [1990] with those given by the closure equation (8) discussed below. However, we have no independent estimates of the fluxes at this level.

For the grid flights we have aircraft data at only one level close to the surface. We took aircraft means at this level (near the base of the mixed layer) as representative of mixed layer averages. We depended on a mixed layer closure equation (8) to give a constraint on the inversion level

buoyancy flux and on the soundings to give the inversion level Bowen ratio.

Mixed Layer Depth

The ABL depth was chosen as the base height of the inversion, Z_i, determined from the radiosonde ascents. There were typically 2–3 ascents at about hourly intervals near the time of each flight, so these values were averaged and an error was estimated from their variability [*Betts et al.*, this issue]. This method of financing Z_i is not accurate: it is an appreciable source of error in the analyses. Single vertical profiles through the ABL take only 5–10 min, and they do not average over the considerable spatial variability. Typically, the ABL is growing with time, but fluctuations of ABL depth associated with mesoscale eddy structures or with the advection of different air masses over the network do occur. On some days, estimates of inversion base height are also available from a single vertically pointing sodar. Maps of the inversion base by lidar would give a better mean, but these are not yet generally available because of the data processing requirements.

Inversion Level Bowen Ratio

Define a simplified notation for the θ and q fluxes in watts per square meter:

$$F_\theta = \bar{\rho} C_p \overline{w'\theta'} \tag{6a}$$

$$F_q = \bar{\rho} L \overline{w'q'} \tag{6b}$$

Both terms in $F_{i\xi}$ in (4′) involve the coupling of the θ and q gradients just below and through the inversion, where the entrainment is taking place. So we can define an inversion level Bowen ratio β_i as

$$\beta_i = F_{i\theta}/F_{iq} = (C_p/L)(\partial\bar{\theta}/\partial\bar{q})_i \tag{7}$$

This Bowen ratio, β_i, was estimated from the radiosonde ascents by plotting (θ, q) mixing diagrams [*Betts*, 1985; *Betts et al.*, this issue]. Aircraft legs in the inversion would give a better mean estimate of β_i, but these were not available in 1987. In some cases there were sudden changes of β_i between soundings. These changes were associated with the disappearance, for example, of a dry layer, as it was completely entrained into the ABL. The mixed layer $\partial\langle\bar{q}\rangle/\partial t$ typically showed an abrupt change from drying to moistening in such a case.

Closure Equation for Inversion Level Fluxes

Dry mixed layer models [*Betts*, 1973; *Carson*, 1973; *Tennekes*, 1973] relate the inversion base virtual heat flux to the surface virtual heat flux, using a closure parameter A_R

$$F_{i\theta_v} = -A_R F_{s\theta_v} \tag{8}$$

Here F denotes a heat flux in watts per square meter. The virtual heat fluxes in energy units are related to the heat and moisture fluxes given by (6), with slight approximation [*Deardorff*, 1980]

$$F_{s\theta_v} = F_{s\theta} + \delta \in F_{sq} \tag{9a}$$

$$F_{i\theta_v} = F_{i\theta} + \delta \in F_{iq} \tag{9b}$$

where $\delta\in = 0.608 C_p T/L \approx 0.07$ and T is temperature. Substituting the Bowen ratio β_i at the inversion from (7), and a similar equation for the surface,

$$\beta_s = F_{s\theta}/F_{sq} \tag{7′}$$

gives the inversion level fluxes of sensible heat and latent heat as

$$F_{i\theta} = -A_R F_\theta (1 + \delta \in /\beta_s)/(1 + \delta \in /\beta_i), \tag{10a}$$

$$F_{i\theta} = F_{i\theta}/\beta_i \tag{10b}$$

The surface heat flux and β_s were found from an average of the surface flux stations, and β_i is from (7).

The terms in parentheses in (10a) come from the density effects of water vapor and hence the latent heat flux, because (8) is expressed in terms of virtual heat flux. These terms are ≈ 1 for large Bowen ratios. The parameter A_R was introduced as a simple closure for the buoyant energy available after dissipation for the entrainment of inversion level air [*Betts*, 1973; *Carson*, 1973; *Tennekes*, 1973; *Stull*, 1976]. Since both inversion level fluxes are proportional to A_R, it is a crucial parameter for budget studies. The works cited suggested $A_R \approx 0.2$, and this has generally been regarded as a satisfactory value for free convective layers in the absence of shear. However, *Betts et al.* [1990], using a set of six FIFE 1987 flights in high wind regimes, found a significantly larger estimate of $A_R = 0.43(\pm 0.12)$. *Betts et al.* [this issue], analyzing a different set of eight flights for FIFE 1987 (only half with strong winds), again found that a large value of $A_R = 0.38\ (\pm 0.16)$ gave sensible and latent heat fluxes at the inversion, which best satisfied the budget equation (4′). Although it is possible that turbulence generated by shear is contributing significantly to the entrainment on some days, even the low wind cases gave values of $A_R \approx 0.4$.

GRAPHICAL SOLUTIONS

Vector Representation of Energy Budgets

Betts [1984] presented mixed layer budgets in two-dimensional vector form, using conserved variable diagrams. These diagrams are particularly helpful for the depiction of the diurnal cycle of the dry mixed layer over land, so the theory will be presented. To simplify the notation from that used in the previous sections, a mixed layer mean will be denoted by just the suffix m. Vector changes for the mixed layer (over some time interval, Δt, such as 1 hour) can be considered as vectors on a (θ, q) diagram (Figure 2).

$$\Delta\xi_m = \Delta(C_p\theta,\ Lq)_m \tag{11}$$

Substituting a vector notation **F** for the two fluxes in (5), and dropping horizontal advection, transforms the budget equation (4′) into a one-dimensional finite difference equation for the time interval Δt,

$$\rho_m(\Delta\xi_m/\Delta t) = (\mathbf{F}_s - \mathbf{F}_i)/Z_i \tag{12}$$

This can be rewritten as

$$\Delta\xi_m = (\mathbf{F}_s - \mathbf{F}_i)/\Omega \tag{13}$$

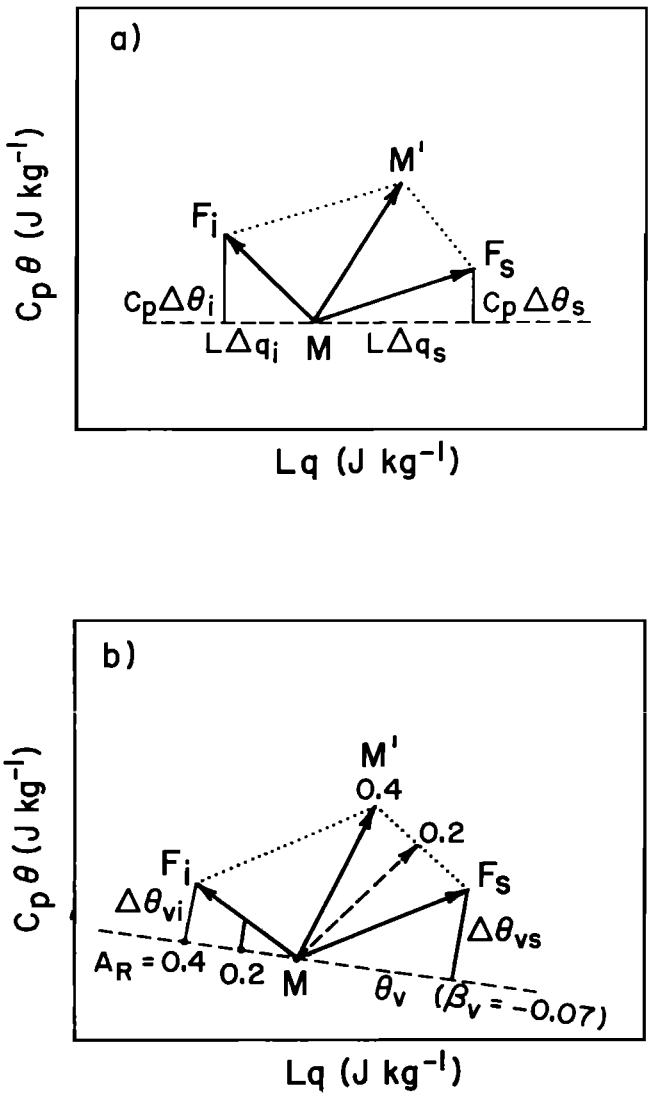

Fig. 2. Vector diagrams for mixed layer θ, q, and θ_v budgets.

where a scaling parameter has been defined (with mass flux units)

$$\Omega = \rho_m Z_i/\Delta t \tag{14}$$

The final step is to rewrite (13) as

$$\Delta\xi_m = \Delta\xi_s - \Delta\xi_i \tag{15}$$

where the fluxes are now represented by vectors in ($C_p\theta$, Lq) space

$$\Delta\xi_s = \mathbf{F}_s/\Omega \tag{16a}$$

$$\Delta\xi_i = \mathbf{F}_i/\Omega \tag{16b}$$

Figure 2*a* illustrates (15). The vector change for the mixed layer from **M** to **M**′ in time Δt is the sum of the effects of the surface flux vector and the entrainment flux vector.

It is clear from (7′) or (11) that the slope of the flux vectors in Figure 2 is associated with a Bowen ratio. Note that the surface flux vector has a positive Bowen ratio, associated with warming and moistening, while the entrainment flux has a negative Bowen ratio, also associated with warming and drying. As mentioned earlier, *Betts et al.* [1990, this issue] used the slope of rawinsonde (θ, q) plots through the capping inversion to determine β_i, the slope of the inversion flux vector. *Betts et al.* [this issue], *Sugita and Brutsaert* [1990], and *Smith et al.* [1991] also noted that the (θ, q) profiles from soundings through the surface superadiabatic layer (below 100 m) gave good estimates of the surface Bowen ratio, in agreement with surface flux measurements.

Figure 2*b* shows the relationship of the closure parameter A_R to the magnitude of the inversion flux vector. The dotted curve is the slope of the dry virtual adiabat [*Betts and Bartlo*, 1991]; it has a slope (corresponding to a Bowen ratio) of $\beta_v = -\delta\in = -0.07$ (the coefficient in equations (9*a*) and (9*b*). Equation (8), in terms of virtual heat flux or virtual potential temperature, can be visualized by projecting the vectors $\mathbf{F}_s$ and $\mathbf{F}_i$ on to the dry virtual adiabat shown. The θ_v fluxes are related to the differences of θ_v.

$$F_{s\theta_v} = \Omega C_p \Delta\theta_{vs} \tag{17a}$$

$$F_{i\theta_v} = \Omega C_p \Delta\theta_{vi} = -A_R F_{s\theta_v}$$
$$\therefore \Delta\theta_{vi} = -A_R \Delta\theta_{vs} \tag{17b}$$

The significance of the magnitude of A_R is clear graphically: we show two values, $A_R = 0.2$ and 0.4. For the same surface heat fluxes and β_i these give the dashed and solid resultant changes of mixed layer, **MM**′ in Figure 2*b*. Larger A_R means more entrainment, with more heating and less net moistening of the mixed layer. The scaling parameter Ω, defined by (14), increases as the mixed layer deepens, so that the vectors $\Delta\xi_s$, $\Delta\xi_i$ decrease in relation to the fluxes they represent (the fluxes themselves have a strong diurnal cycle as well). Changes in the mixed layer due to horizontal advection can be added to Figure 2 as an additional vector, say, $\Delta\mathbf{M}_{ad}$ in time Δt, as done by *Betts* [1984].

Idealized ABL Heat and Moisture Budgets

The case studies discussed by *Betts et al.* [1990, this issue] generally support the use of simple mixed layer models. Together, these studies give a good conceptual picture of the transition in the ABL daytime heat and moisture budget from summer to fall. This understanding is important for the modeling objectives of FIFE.

If we ignore horizontal advection as a climatological simplification, since it varies in magnitude and direction from day to day, the mixed layer model can be used to give idealized one-dimensional solutions for the rise of θ and q in terms of surface and inversion level Bowen ratios and the entrainment coefficient A_R. The local changes of mixed layer θ and q are given by

$$C_p \partial\theta_m/\partial t = (F_{s\theta} - F_{i\theta})/\rho_m Z_i \tag{18a}$$

$$L\partial q_m/\partial t = (F_{sq} - F_{iq})/\rho_m Z_i \tag{18b}$$

Substituting from (10*a*) and (10*b*) for the inversion level fluxes and for the surface Bowen ratio gives, after rearrangement,

$$C_p \partial\theta_m/\partial t = (F_{s\theta}/\rho_m Z_i)[1 + A_R(1 + .07/\beta_s)/(1 + .07/\beta_i)] \tag{19a}$$

$$L\partial q_m/\partial t = (F_{sq}/\rho_m Z_i)[1 + A_R(\beta_s + .07)/(\beta_i + .07)] \quad (19b)$$

The first terms in (19*a*) and (19*b*) are just the tendency of the surface fluxes to warm and moisten the ABL. If we were to make the simple (but wrong) assumption of zero fluxes at the inversion, these are the sole terms in the one-dimensional ABL budget. The second pair of terms, proportional to A_R, are from the entrainment fluxes of typically warm, dry air at the inversion. Our finding that $A_R \approx 0.4$ (not 0.2, as often used in models) is of quantitative significance here. It means that the entrainment fluxes are rather large. These A_R terms in (19*a*) and (19*b*) look deceptively similar. However, in the $\partial\theta/\partial t$ formula the multiplier on A_R is always positive, and it is typically between 1 and 2, decreasing from summer to fall as β_s increases. As a result, $C_p\partial\theta_m/\partial t \approx 1.7\ F_{s\theta}/\rho_m Z_i$, decreasing a little from summer to fall. This flux convergence always warms the ABL during the day, and it increases with the increase of $F_{s\theta}$ in the fall. In contrast, in (19*b*) the weighting on the inversion level moisture flux is the same expression, multiplied by β_s/β_i, which is typically negative and increases greatly from summer to fall, as the vegetation dies and the surface heat flux, which drives entrainment, increases. As a result, $\partial q_m/\partial t$ can easily change sign. For typical summer values of $(\beta_s, \beta_i) = (0.3, -0.3)$ from *Betts et al.* [this issue], we get

$$L\partial q_m/\partial t \approx 0.28\ F_{sq}/\rho_m Z_i \quad (20a)$$

while for the fall values of $(\beta_s, \beta_i) = (4, -0.5)$, we get

$$L\partial q_m/\partial t \approx -3.2\ F_{sq}/\rho_m Z_i \quad (20b)$$

In this example, the entrainment flux in summer reduces the ABL moistening to about a third of the tendency of the surface latent heat flux, whereas in the fall the drying from the entrainment at the inversion can be 4 times the moistening owing to the weak surface evaporation, so that it dominates in the budget. This is in fact the mechanism through which the ABL dries out in the fall, after the death of vegetation, as it tries to reach a new climatic equilibrium. Note that dividing (19*a*) by (19*b*) shows that the direction of MM′ is not sensitive to Z_i for given β_s, β_i.

The crossover of $\partial q_m/\partial t = 0$ is of conceptual importance. Equation (19*b*) gives the critical surface Bowen ratio, $\beta_{sc}(q)$, for which $\partial q_m/\partial t = 0$, as a function of β_i

$$\beta_{sc}(q) - \beta_v = -(\beta_i - \beta_v)/A_R \quad (21)$$

where $\beta_v = -\delta\in = -0.07$ is again the Bowen ratio corresponding to the slope of the dry virtual adiabat. In fact, (21) can be derived directly from Figure 2*b* if the vector MM′ is at constant q (with only the small approximation of $\theta_v/\theta \approx 1$).

Figure 3 shows the critical surface Bowen ratio given by (21) as a function of inversion level Bowen ratio, for a range of values of the entrainment parameter A_R. On these curves the surface evaporation just balances the entrainment of dry air at the inversion, as is often observed. For surface Bowen ratios to the left and below the curves in Figure 3 the ABL will moisten and vice versa. The physical importance of the lack of certainty in entrainment rates is apparent from Figure 3. For example, for the typical inversion level Bowen ratio of −0.3 shown, the critical surface Bowen ratio for no moistening of the ABL rises from 0.39 to 1.08 as the entrainment parameter falls from 0.5 to 0.2.

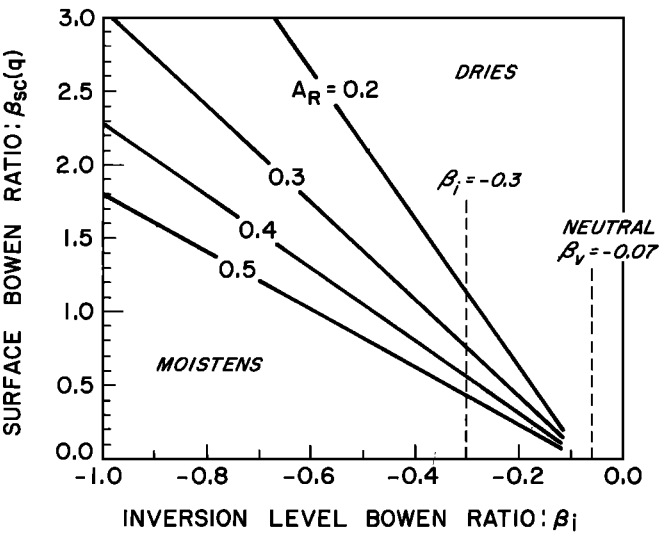

Fig. 3. Critical surface Bowen ratio for $\partial q_m/\partial t = 0$ as a function of inversion level Bowen ratio and entrainment parameter, A_R.

Another solution of physical importance is the change of ABL equivalent potential temperature with time, $\partial\theta_{Em}/\partial t$. Expand a change in θ_E as

$$(\theta/\theta_E)\delta\theta_E = \delta\theta + (L\theta/C_pT)\delta q \quad (22)$$

so that the wet adiabat (shown by a subscript w) corresponds to a Bowen ratio

$$\beta_w = (C_p/L)(\partial\theta/\partial q)_{\theta_E} = -(\theta/T) \approx -1 \quad (23)$$

in the ABL. An expression similar to (21) for the critical Bowen ratio, $\beta_{sc}(\theta_E)$, is there obtained for $\partial\theta_{Em}/\partial t = 0$ by combining (18), (22), and (23)

$$(\beta_{sc}(\theta_E) - \beta_w)/(\beta_{sc}(\theta_E) - \beta_v) = -A_R(\beta_i - \beta_w)/(\beta_i - \beta_v) \quad (24)$$

where β_w, $\beta_v = -1$, -0.07 in the ABL. Figure 4 shows the curves for the critical $\beta_{sc}(\theta_E)$ given by (24), for a range of A_R values. These increase much more steeply than $\beta_{sc}(q)$, since the required solution for ABL $\partial\xi/\partial t$ now has the slope of $\beta_w \approx -1$ in Figure 2 (that of constant θ_E). The rise or fall of θ_E in the daytime ABL is important to the stability of the atmosphere to deep convection, particularly during the occurrence of thunderstorms. We can see from Figure 4 that for typical $\beta_i \approx -0.3$, θ_E will generally rise over moist terrain in the daytime ABL. The FIFE experiment will give some understanding of the seasonal transition in the surface processes that control β_s. The inversion level Bowen ratio β_i is, however, influenced by processes in the free atmosphere. It depends on the coupling between the θ and q gradients through the capping inversion at the top of the ABL. In summer, the atmospheric thermodynamic profiles have usually been previously modified by moist convection through deep layers or, in some cases, by dry convection over warm elevated terrain. This places constraints on $(\partial\bar{\theta}/\partial\bar{q})$ just above the ABL. The profile must be more stable than the dry neutral threshold of $\beta_v = -0.07$. Moist

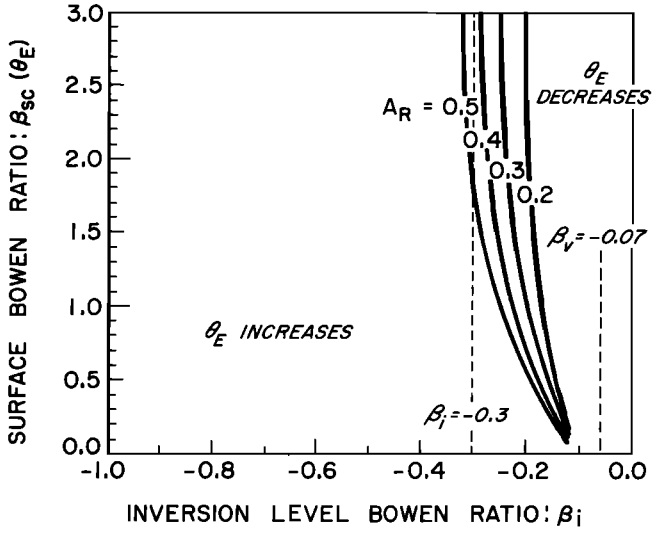

Fig. 4. Critical surface Bowen ratio for $\partial\theta_{Em}/\partial t = 0$.

cumulus convection typically requires or generates a more unstable ($\partial\overline{\theta}/\partial\overline{q}$) structure than the wet adiabat, which has $\beta_w \approx -1$, and the wet virtual adiabat, which has $\beta_{wv} \approx -0.8$. Generally, we find in the cumulus cloud layer that $-0.3 > \beta > -0.5$ [*Betts and Boers*, 1990]. The predominance of values of β_i in this range in the FIFE data results from the prior conditioning of the lower troposphere by cumulus convection. In some cases, however, particularly in the fall when the ABL is dry, the advection of moist layers over the FIFE site can produce any value of β_i.

A different situation exists in the early to midmorning, as the nocturnal inversion is removed. The ABL may then grow rapidly into a preexisting residual mixed layer from the previous day's dry convection. These may have relatively unstable structures, with β_i in the range $-0.07 > \beta_i > -0.3$. These less stable values of β_i are also found in the atmosphere preceding severe storms [e.g., *Betts*, 1984], where deep dry mixed layers formed previously over elevated terrain often overlay and cap a shallow moist ABL [e.g., *Ludlam*, 1980].

Two conclusions can be reached. First, knowledge of the overlying atmospheric structure is important. Second, understanding and modeling the link between the ABL inversion level fluxes and the surface fluxes is fundamental to predicting daytime time trends within the ABL. Our budget studies suggest that this can be done with simple mixed layer models. The uncertainty in the value of the entrainment closure parameter A_R clearly suggests the need for further studies of ABL deepening by entrainment. The incorporation of the whole diurnal cycle into a simple one-dimensional mixed layer model would enable us to study the seasonal changes in the diurnal cycle, as a function of surface vegetative processes and free atmospheric parameters. One additional parameter, which is not measured, is the mean subsidence field, but on climate time scales there are strong links to the radiative field [*Betts and Ridgway*, 1988, 1989], which might perhaps also be applicable in subsiding regions over the continents.

Discussion of Aircraft Budget Results

Detailed analyses of the FIFE 1987 stack and grid flights are given by *Betts et al.* [1990, this issue]. *Grossman* [this issue] presents a budget analysis of L-shaped patterns in June. *Kelly et al.* [this issue] intercompare surface and extrapolated aircraft flux measurements. Important conclusions are summarized here, and recommendations are made for future experiments. The mixed layer budget model proved very useful both in intercomparing different data and in determining vertical gradients.

Comparison of Surface and Aircraft Measurements

The aircraft generally underestimate the sensible and latent heat fluxes, when compared with an average of the surface flux sites, after using vertical flux gradients in the ABL to convert to the same level. In the work by *Betts et al.* [1990] it appeared that the aircraft flux underestimate for the Canadian Twin Otter was more than 30%. However, the difference has narrowed after subsequent correction of the data. The mean surface fluxes have been reduced following a recalibration of the net radiometers used by many of the Bowen ratio flux sites. In addition, *MacPherson* [1990] found that reprocessing of the Twin Otter aircraft fluxes using only the Litton inertial navigation system increased the fluxes from that aircraft by 13%. *Betts et al.* [this issue] estimated that the residual flux underestimate in 1987 for the Canadian Twin Otter was about 20% for the heat and moisture fluxes. *Kelly et al.* [this issue] found similar flux underestimates for both the Twin Otter and the Wyoming King Air aircraft. The is of the order expected from the high-pass filtering of the data at 0.012 Hz [*Desjardins et al.*, this issue], and the undersampling of long wavelengths, because the FIFE runs were only 15 km in length. However, it appears that in October the aircraft latent heat fluxes, although small ($\approx$70 W m^{-2}), are larger than the surface site mean. This needs further study. It is possible that the surface sites are less representative after most of the vegetation has died (for example, more evapotranspiration in the gulleys), but *Betts et al.* [this issue] suggested that there appeared to be a significant bias in the surface flux data in October, with the mean surface latent (sensible) heat fluxes being low (high) by about 30 W m^{-2}. There may be some systematic errors in the Bowen ratio site measurements when the Bowen ratio is large (E. A. Smith, personal communication, 1991).

The aircraft underestimate due to filtering and sampling seems now fairly well understood. In future experiments it seems advisable to archive unfiltered, detrended, and filtered data, when aircraft averages are to be compared with surface averages. In addition, longer flight legs are desirable to reduce the undersampling of the long wavelength contribution to the fluxes. Over land, however, inhomogeneities in space may set limits on pattern size, and the separation of time and space derivatives may require the assumption of linearity in time for the duration of a flight pattern.

Validity of Mixed Layer Models

The budgets are generally consistent with mixed boundary layer theory. Above the surface superadiabatic layer (depth less than 100 m) the experimental data show nearly well mixed layers with little vertical variation in the time rates of change or horizontal gradients, in agreement with the mixed layer model approximation. As a result, the grid flights at a single level give a useful depiction of time and space gradients for the mixed layer.

ABL Top Entrainment

The somewhat surprising result of great importance to FIFE is that the inversion level fluxes due to ABL top entrainment appear to be about double those used in many simple mixed layer closure models. *Betts et al.* [1990] estimated a mixed layer closure parameter $A_R = 0.43 \pm 0.12$, and *Betts et al.* [this issue] found 0.38 ± 0.16; where the long accepted value for free convective boundary layers has been $A_R \approx 0.2$ [*Stull*, 1988]. Although some flight days had strong winds, when turbulence generated by surface shear might be expected to drive additional entrainment, others with high entrainment had light winds. The impact of this greater entrainment is threefold: the ABL grows more rapidly, warms more rapidly, and entrains dry air more rapidly. This has a big impact on the ABL moisture budget. When the surface moisture flux is large, as in the summer, it reduces the moistening of the ABL; and when the surface moisture flux is low, as in the fall, it produces a drying of the ABL during the day. Further studies of entrainment rates are needed, using continuous surface based lidar or sodar measurements of ABL height. One major improvement in measurement strategy would be to measure both inversion height and strength using a wind profiler radar, with an added radio acoustic sounding system (RASS) to provide the temperature profiles. It is clear that better methods of measuring either boundary layer growth or the vertical gradients of the convective fluxes are needed to resolve the uncertainties in the ABL top entrainment rates.

Advantages of Specific Flight Patterns

A variety of aircraft patterns were flown during FIFE. Some of the 1987 L-shaped patterns and much of the 1989 aircraft data have not yet been analyzed from a budget perspective. Nonetheless, the FIFE budget studies completed so far suggest several conclusions about measurement strategy for the daytime ABL. In the budget equation (4′) there are three key terms: (1) the time derivative, (2) the horizontal advection term, and (3) the vertical flux gradient. A single aircraft, flying any pattern, can measure the mean time derivative quite well and can estimate the space derivative along the track from trend lines, provided enough legs are flown. The major issue in budget analyses is how to determine horizontal advection and the vertical flux gradients at the same time. The cross-track horizontal advection was found by *Betts et al.* [1990, this issue] by separating a mean north-south spatial derivative by assuming linear gradients in time. This assumption is not always satisfied. In two afternoon flights, which spanned the surface temperature maximum, the nonlinearity of $\partial\overline{\theta}/\partial t$ introduced significant errors into the estimate of the north-south advection. We recommend that flights be made nearer local noon when the rise of temperature is more linear. Supporting data from the surface stations is essential for assessing nonlinearity in time, and frequent soundings are needed to show changes in ABL-top Bowen ratio. In both *Betts et al.* [1990] and *Betts et al.* [this issue], we found that a single aircraft could estimate the horizontal advection on the 15-km scale of the FIFE network, but only if the gradients in time and space remained approximately constant during a flight. The error in measuring the north-south advection in high (north or south) winds is, however, quite large with a north-south pattern dimension of only 10–15 km. This along-wind horizontal advection needs a larger spatial distance than was typical of FIFE to achieve an accuracy comparable with the time derivative. The grid pattern gives better horizontal structure than the stack pattern (but no vertical structure). The repeated minigrid pattern has a clear advantage in separating the time and space derivatives using a single aircraft, because the pattern associated with advection is repeated. In general, it would be desirable to have two aircraft to study the diurnal cycle: one flying a fixed pattern in space, such as a crosswind racetrack from surface to inversion or a stack of at least three levels in the vertical, to measure the time and height dependence; and a second flying a low level grid pattern to resolve the horizontal spatial structure and the other space derivative. The problem with depending on two aircraft to get a complete data set is that all instruments on both planes must perform adequately.

CONCLUSIONS

The FIFE analyses have shown the importance of the FIFE network of integrated observations. The aircraft monitor the changing structure of the mixed layer. The sonde data give the crucial inversion depth and the estimate of the inversion level Bowen ratio. Sudden changes in entrainment at the inversion are reflected in both the aircraft and the surface data [*Betts et al.*, this issue]. The comparison of the aircraft and surface time trends showed us cases where the aircraft pattern included sudden transistions and the gradients did not satisfy linearity conditions in time. The FIFE budget studies have shown that while the aircraft flux estimates give a good horizontal distribution [*Schuepp et al.* 1990], they must be corrected for the flux underestimates due to filtering and undersampling at long wavelengths. Mixed layer models can be used for the growth of the cloud-free ABL over the FIFE network with some confidence and with some awareness of the variability associated with horizontal advection and changes in the thermodynamic properties of the air entrained at the inversion. These studies also suggest, however, that ABL top entrainment may be underestimated significantly in many parametric models.

Acknowledgments. A. K. Betts was supported by NASA-GSFC under contract NAS5-30524 and by NSF under grant ATM90-01960. Two reviewers improved the clarity of the paper.

REFERENCES

Betts, A. K., Non-precipitating cumulus convection and its parameterization, *Q. J. R. Meteorol. Soc.*, *99*, 178–196, 1973.

Betts, A. K., Reply to Deardorff et al. (1974), *Q. J. R. Meteorol. Soc.*, *10*, 469–472, 1974.

Betts, A. K., Boundary layer thermodynamics of a high plains severe storm, *Mon. Weather. Rev.*, *112*, 2199–2211, 1984.

Betts, A. K., Mixing line analysis of clouds and cloudy boundary layers, *J. Atmos. Sci.*, *42*, 2751–2763, 1985.

Betts, A. K., and J. Bartlo, The density temperature and the dry and wet virtual adiabats, *Mon. Weather Rev.*, *119*, 169–175, 1991.

Betts, A. K., and R. Boers, A cloudiness transition in a marine boundary layer, *J. Atmos. Sci.*, *47*, 1480–1497, 1990.

Betts, A. K., and W. Ridgway, Coupling of the radiative, convective and surface fluxes over the equatorial Pacific, *J. Atmos. Sci.*, *45*, 522–536, 1988.

Betts, A. K., and W. L. Ridgway, Climatic equilibrium of the atmospheric convective boundary layer over a tropical ocean, *J. Atmos. Sci.*, *46*, 2621–2641, 1989.

Betts, A. K., R. L. Desjardins, J. I. MacPherson, and R. D. Kelly,

Boundary layer heat and moisture budgets from FIFE, *Boundary Layer Meteorol.*, *50*, 109–137, 1990.

Betts, A. K., R. L. Desjardins, and J. I. MacPherson, Budget analysis of the boundary layer grid flights during FIFE 1987, *J. Geophys. Res.*, this issue.

Carson, D. J., The development of a dry inversion-capped convectively unstable boundary layer, *Q. J. R. Meteorol. Soc.*, *99*, 450–467, 1973.

Deardorff, J. W., Prediction of convective mixed-layer entrainment for realistic capping inversion structure, *J. Atmos. Sci.*, *36*, 424–436, 1979.

Deardorff, J. W., Cloud-top entrainment instability, *J. Atmos. Sci.*, *37*, 131–147, 1980.

Deardorff, J. W., G. E. Willis, and D. K. Lilly, Comments on Betts [1973], *Q. J. R. Meteorol. Soc.*, *100*, 122–123, 1974.

Desjardins, R. L., P. H. Schuepp, J. I. MacPherson, and D. J. Buckley, Spatial and temporal variation of the fluxes of carbon dioxide and sensible and latent heat over the FIFE site, *J. Geophys. Res.*, this issue.

Grossman, R. L., Convective boundary layer budgets of moisture and sensible heat over an unstressed prairie, *J. Geophys. Res.*, this issue.

Kelly, R. D., E. A. Smith, and J. L. MacPherson, A comparison of surface sensible and latent heat fluxes from aircraft and surface measurements in FIFE 1987, *J. Geophys. Res.*, this issue.

Ludlam, F. H., *Clouds and Storms*, 405 pp., Pennsylvania State University Press, University Park, 1980.

MacPherson, J. I., Wind and flux calibrations on the NAE Twin Otter, *NRC, NAE Lab. Tech. Rep.*, *LTR-FR-109*, Inst. for Aerosp. Res., Ottawa, Ont., Canada, Feb. 1990.

Schuepp, P. H., R. L. Desjardins, J. I. MacPherson, and M. Y. Leclerc, Footprint prediction of scalar fluxes: Reliability and implications for airborne flux measurements over the FIFE site, paper presented at the American Meteorological Society Symposium on FIFE, Anaheim, Calif., Feb. 7–9, 1990.

Smith, E. A., H. J. Cooper, W. L. Crosson, and D. D. Delorey, Retrieval of surface heat and moisture fluxes from slow launched radiosondes, *J. Appl. Meteorol.*, *30*, 1613–1626, 1991.

Smith, E. A., et al., Area-averaged surface fluxes and their time-space variability over the FIFE experimental domain, *J. Geophys. Res.*, this issue.

Stull, R. B., The energetics of entrainment across a density interface, *J. Atmos. Sci.*, *33*, 1260–1267, 1976.

Stull, R. B., *An Introduction to Boundary Layer Meteorology*, 666 pp., Kluwer Academic, Boston, Mass., 1988.

Sugita, M., and W. Brutsaert, How similar are temperature and humidity profiles in the unstable boundary layer?, *J. Appl. Meteorol.*, *29*, 489–497, 1990.

Tennekes, H., A model for the dynamics of the inversion above a convective boundary layer, *J. Atmos. Sci.*, *30*, 558–567, 1973.

A. K. Betts, Atmospheric Research, R.D. 2, Box 3300, Middlebury, VT 05753.

(Received February 7, 1991;
revised November 29, 1991;
accepted December 16, 1991.)